Reprinted from I&EC RESEARCH, 1990, 29, 171.

Fast Catalytic Cracking of Heavy Gas Oils: Modeling Coke Deactivation

M. Larocca
Du Pont Research Centre, Du Pont Canada, Kingston, Ontario, Canada K7L 5A5

S. Ng
Energy Research Laboratories, CANMET, Ottawa, Ontario, Canada K1A 0G1

Hugo de Lasa*
Chemical Reactor Engineering Centre, Faculty of Engineering Science, The University of Western Ontario, London, Ontario, Canada N6A 5B9

An unsteady-state pulse technique has been used to evaluate kinetic parameters for catalytic cracking of heavy gas oil with steamed commercial catalysts. The method closely mimic conditions of commercial FCC riser reactors. The experimental results obtained at a catalyst time-on-stream of under 20 s allowed the evaluation of activation energies and kinetic constants for gas oil decomposition into gasoline and light gas plus coke, as a whole, as well as for individual groups: paraffins, naphthenes, and aromatics. Two models were considered in the present study: (a) a three-lump model featuring gas oil, gasoline, and gas plus coke; (b) a five-lump model, where gas oil was split into paraffins, naphthenes, and aromatics. It was found that the catalyst deactivation due to coke formation, for contact times under 20 s, can be represented by both an exponential decay function and a power decay function with an average exponent of 0.1–0.2.

1. Introduction

Catalytic cracking of gas oils for gasoline production is one of the most important processes in petroleum refining, because of the strategic and economic value of its products (de Lasa, 1982). During reaction, the cracking catalyst deactivates due to the formation and deposition of coke, which severely affects the catalyst performance. Process optimization under catalyst decay is an engineering problem that requires a knowledge of the catalyst deactivation kinetics (Wolf and Alfani, 1982). The quantification of the decay phenomenon has been attempted in several ways by researchers during the past years (Wojciechowski, 1974; Wheeler, 1955; Froment and Bischoff, 1961, 1962).

A popular type of theory on deactivation is based on the time-on-stream concept. Practically all researchers have used this model to formulate various empirical functions which were then used to account for the decay of the activity of the catalyst (Meisenheimer, 1962; Gross et al., 1974; Newson, 1975; Nace, 1969a,b, 1970; Mann et al., Mann and Thomson, 1987; Tan and Fuller, 1970; Voltz et al., 1971; Nalltham and Tarrer, 1983; Weekman, 1968; Voorhies, 1945; Wojciechowski, 1968, 1974; Forzatti et al., 1984; Fuentes, 1985; El-Kady and Mann, 1982a,b; Corella et al., 1985; Habib et al., 1977). More recently, a partitioned flow model was introduced by Dean and Dadyborjor (1989) to distinguish between differences in activities and coke levels in the matrix and in the zeolite.

Although most authors agree on the use of the time-on-stream theory, there is no agreement in the specific equation that governs the catalyst deactivation. In fact, the decay has been modeled with linear, exponential, hyperbolic, reciprocal, and power functions to fit the experimental data of the particular researcher. There are generally two functions that fit quite well the experimental data: the power and the exponential functions. Between the two, the latter is the most popular and widely used.

Experimental data fit the exponential decay model very well, starting from a time-on-stream of approximately 1 min. However, in the initial region, the decay behavior follows a function of different decay order or an exponential function with a different decay coefficient (Nace, 1969a,b, 1970; Corella et al., 1985; Habib et al., 1977; Forzatti et al., 1984; Szepe and Levenspiel, 1971; Fuentes, 1985; Weekman, 1968, 1979; Voltz et al., 1971; Jacob et al., 1976; Collyer et al., 1988). Because bench-scale reactors usually used for these experiments are designed for collecting data for large values of catalyst time-on-stream (1 min or higher), only a few points are normally measured before the first minute. Since the majority of data were taken by different researchers at values of catalyst time-on-stream higher than 1 min, the first-order decay model (single-exponential function) fits the experimental data quite well. This phenomenon is extremely important if one considers that riser reactors operate with a contact time that is smaller than 20 s, due to the high catalyst activity.

In this experimental study, a reacting pulse technique is used, which does not suffer the limitation of the conventional reacting systems traditionally used for catalytic cracking studies, allowing for a cumulative hydrocarbon–catalyst contact time lower than 20 s.

2. Experimental Section

The pulse technique uses a small pulse of vaporized gas oil which is circulated through a small amount of catalyst. The products of reaction are analyzed on-line through a gas chromatograph and a mass spectrometer. The apparatus for the experimental work is presented in Figure 1.

The carrier gas, helium, was circulated through a drierite filter and a molecular sieve filter (A) to remove any moisture and impurities. The helium flow was introduced into the main system through a Matheson 9240 Model 8100 mass flow controller (B), specially calibrated for helium gas. The helium flow was circulated through a metal blox (C) containing thermal conductivity detectors (TCD). Two TCD detectors were installed inside this box to check the shape of the inlet and outlet hydrocarbon pulses. Helium passed first through the reference side of the two detectors, and then it circulated through a six-port gas injection valve (D) and a bypass valve (E). The gas finally reached the hydrocarbon injection system (G). A 10-μL syringe was used to inject the gas oil pulse directly into the heated metal block (G). With this end, a chromatographic septum was installed next to the heated block such that the needle could be introduced in a cavity inside the block where the vaporization of the hydrocarbon occurred instantaneously.

* Author to whom correspondence should be addressed.

0888-5885/90/2629-0171$02.50/0

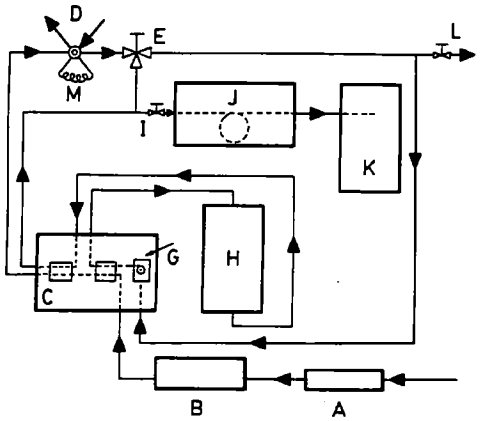

Figure 1. Schematic diagram of experimental apparatus: (A) filter, (B) flow control, (C) TCD box, (D) six-port valve, (E) three-way valve, (G) syringe injector, (H) reactor, (I) high-temperature valve, (J) gas chromatograph, (K) mass spectrometer, (L) vent valve, (M) gas loop.

The block was kept at high temperature with a firerod 300-w capacity. The reactant pulse was then monitored by the first TCD detector prior to its introduction into the reacting system (H), from the top of the reactor. The reacted and unreacted hydrocarbon pulses were then carried by the helium stream into the second TCD detector and then circulated through a high-temperature valve (I) and finally into the gas chromatograph (J) for on-line analysis. Then, the same helium stream was used as carrier flow and for the gas chromatograph. The gas chromatograph used was equipped with a glass capillary inlet splitter. This splitter with a 1/50–1/100 splitting ratio was used to "split" the pulse into two unequal portions, the smaller one went to the capillary column (HP-1) for analysis, preventing in this way column overloading. The gas chromatograph was programmed as follows: 30 °C for 3 min plus a rate of 16 °C/min until 320 °C. This temperature programming allowed detection simultaneously of most of the light gases, gasoline, cycle oil, and unconverted gas oil in a single chromatogram.

During the fluidization period, taking place between injections to mix the catalyst bed and to prevent the development of coke profiles, the flow was reversed by means of valves E, I, and L. Furthermore, for gas calibration injection, valve positions were set in order to allow the calibrating gas to fill loop M. The six port valve (D) was then used to inject the gas into the system. During this operation, valves I and E were set to bypass the reactor and direct the flow to the gas chromatograph.

All fluid transporting tubings used in the setup were 314 stainless steel with a diameter of 0.765 mm. These tubes were enclosed in 4-mm tubing.

The reactor itself consisted of a downflow vertical-cylindrical arrangement, with a diameter of 8 mm and a total height of 40 mm, filled with 0.1 g of catalyst diluted with 2.3 g of inerts (Exolon-fused alumina). The particles were confined in the bed by two porous grids with 20-μm openings.

The catalysts used, listed in Table I were steamed in a fluid bed reactor at 1039 K and atmospheric pressure with 100% steam for 18 h. An approximately 40% surface area loss confirmed the desired "equilibrium" conditions. Feedstock properties are listed in Table II.

Runs were performed at three different carrier helium flows (120 135, and 150 std mL/min) and two temperature levels (783 and 823 K). Each run consisted of 10 pulses of 5 μL of gas oil. Each pulse contacted the catalyst for an average contact time slightly below 2 s. For example,

Table I. Fresh Catalyst Properties

catalyst	SuperNova D	Octacat	Octex	GX-30
nomenclature abbrev	SND	OCT	OTX	GX
Al_2O_3, wt %	45	26	42	34
Na, wt %	0.25	0.22	0.64	0.37
REO, wt %	2.5	>2	1.8	4.5
unit cell size of steamed catalyst (A)	24.30	24.24	24.31	24.40
surface area following steaming at 1039 K during 18 h, m^2/g	155	153	149	126
bulk density, g/cm^3	0.75	0.70	0.80	0.74

Table II. Gas Oil Properties

gas oil	SF[a]	PF[b]
specific gravity	0.9389	0.9039
aniline point, K	332	344
sulfur, wt %	0.24	1.33
nitrogen, wt %	0.102	0.053
volumetric av bp, K	666	640
simulated distillation, K		
IBP	534	482
5 wt %	573	537
10 wt %	595	558
30 wt %	630	609
50 wt %	660	648
70 wt %	696	691
90 wt %	747	743
95 wt %	771	765
FBP wt %	817	817
paraffins, wt %	7.4	75.7
molecular wt	313	280
naphthenes, wt %	40.9	14.6
molecular wt	305	226
aromatics, wt %	51.7	9.7
molecular wt	358	249

[a] Synthetic feedstock. [b] Paraffinic feedstock.

this gave for the 120 std mL/min helium flow and after 10 consecutive injections of gas oil an equivalent cumulative contact time of 19 s and a cumulative catalyst-to-oil ratio ranging from 2 to 10. Moreover, it has to be pointed out that with pulses of 2 s thermal cracking was never greater than 1.5% conversion.

Coke was determined in independent experiments. Following a complete run, about 10 injections of hydrocarbon feedstock, the catalyst was regenerated in the presence of air at 923 K. Coke yields for the 10 hydrocarbon injections were determined by weight difference. Since alumina is highly hydrophilic, special precautions were taken in order to eliminate the water from the sample before weighing. With this end, the sample unloaded from the reactor was heated under controlled conditions (53 K for 2 h) and under ultrapure helium flow (5 cm^3/min).

3. Reactor Modeling

The experimental results were analyzed with two kinetic models: (a) a three-lump model, featuring gas oil, gasoline, and gas plus coke; (b) a five-lump model, where gas oil was split into paraffins, naphthenes, and aromatics.

In the three-lump model, gas oil was considered one single component, which under cracking conditions decomposes into gasoline, gas, and coke. Gasoline overcracking to gas and coke was further included in the model, forming in this way the classical triangular scheme as shown in Figure 2a.

The mathematical model was developed by using three mass balances, one for each lump, under the unsteady-state conditions characteristic of the pulse reaction technique.

The model proposed included the following assumptions: (a) piston flow model, a reasonable simplification, taking into account the special design of the microcatalytic reactor

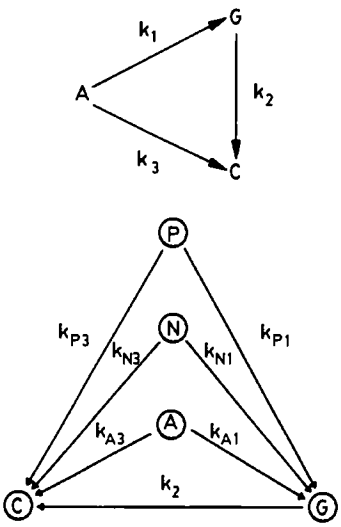

Figure 2. (a, top) Three-lump model. Lump A, gas oil; oil; lump G, gasoline; lump C, light gases (C_1–C_4) plus coke. (b, bottom) Five-lump model. Lump P, paraffinic fraction in gas oil; lump N, naphthenic fraction in gas oil; lump A, aromatic fraction in gas oil; lump G, gasoline; lump C, light gases (C_1–C_4) plus coke.

used and the testing performed with inert tracer injections; (b) constant pressure and temperature, an appropriate hypothesis, considering that pressure drops in the bed were about 2% of the total pressure and the small amounts of hydrocarbon samples involved; (c) second-order reaction for gas oil cracking, a typical order for this type of reaction, confirmed later in the study observing the adequacy of the model to predict the experimental results; (d) adsorption–desorption phenomena at the catalyst surface at equilibrium, a reasonable consideration in view of the relatively small change of shape of the input–output signals recorded by the TCD detectors; (e) constant catalyst activity or the equivalent constant coke concentration in the bed during one pulse, an appropriate simplification taking into account the special device for reversing the flow of carrier gas, allowing fluidization of the bed in between injections.

Under these conditions, the following equation can be proposed for the gas oil cracking:

$$\frac{\partial C_a}{\partial t}[(1-\epsilon)(1-\epsilon_p)K_a\rho_p/\epsilon + (1-\epsilon)\epsilon_p/\epsilon + 1] = -U\frac{\partial C_a}{\partial Z} + r_a\rho_p f(1-\epsilon)(1-\epsilon_p)/\epsilon \quad (1)$$

This equation includes in the left-hand-side an accumulation term of hydrocarbons in the solid phase, in the intraparticle volume, and in the interparticle voidage. The right-hand side of eq 1 includes the addition of two terms. The first one corresponds to the convective transport of hydrocarbons, while the second one represents the consumption or generation of hydrocarbons by catalytic cracking.

This equation is subject, under the pulse reaction experiments, to the following conditions:

$z = 0 \quad t \geq 0 \quad C_a = C_{a0}$ (boundary condition)

$z > 0 \quad t < 0 \quad C_a = 0$ (initial condition)

This indicates that at the reactor inlet the incoming pulse perturbation is known and that a gas oil only proceeds once the previous hydrocarbon perturbation was completely eluted from the catalytic bed. These two conditions were applicable in our study considering that the TCD at the reactor entry gave the shape of the incoming pulse and that the TCD at the reactor exit allowed establishment of the time for complete elution of the products from the reactor.

Similar equations can be written for the gasoline and the gas plus coke lumps. The equations were transformed in a set of ordinary differential equations, using Laplace transforms. It has to be stressed that for the three-lump model the rate of reaction term, r_a, for the gas oil presents a square concentration term. The solution by Laplace transform was made possible through the use of a correction factor, F. This factor is defined as follows:

$$F = \int_0^\infty \exp(-st)\, f(t)^2\, dt \quad (2)$$

where $f(t)$ is the shape of the hydrocarbon pulse, as it is recorded by the thermal conductivity detectors.

The application of the Laplace transform to eq 1 and the consideration of the F factor give

$$\bar{C}_a s - C_a(0) + \frac{d\bar{C}_a}{dz}\frac{U}{D} = -(k_1 + k_3)\bar{C}_a{}^2\frac{FB}{D} \quad (3)$$

with

$$B = \rho_p f(1-\epsilon)(1-\epsilon_p)/\epsilon$$

and

$$D = (1-\epsilon)(1-\epsilon_p)K_a\rho_p/\epsilon + (1-\epsilon)\epsilon_p/\epsilon + 1$$

Similar relationships can be obtained for both gasoline and coke. It has to be pointed out that the reaction terms for coke and gasoline formation from gas oil (second order reactions) involve an F factor. This factor becomes one for gasoline consumption and coke formation from gasoline (first-order reactions).

The equation system was evaluated numerically at the condition $s = 0$. At this condition, the group of parameters multiplying the time derivative in eq 1 cancels. The resulting set of differential equations was solved, converting the derivatives into finite differences. Then, the following equations used for the calculation of the individual theoretical outlet lump concentrations result:

gas oil outlet concentration

$$\bar{C}_a = \bar{C}_{a0}\{[(k_1 + k_3)BF\bar{C}_{a0}\Delta Z/Uv] + 1\}^{-1} \quad (4)$$

where

$$B = \rho_p f(1-\epsilon)(1-\epsilon_p)/\epsilon \quad (5)$$

gasoline outlet concentration

$$\bar{C}_G = B\Delta Z k_1 F S_G \bar{C}_{a0}{}^2(1 - B\Delta Z k_2/U)^{v-1}/U + B\Delta Z k_1 F S_G \bar{C}_{a0}{}^2/U\sum_{j=1}^{v-1}\{(1 - B\Delta Z k_2/U)^{j-1}/[1 + (v - j)B\Delta Z F\bar{C}_{a0}(k_1 + k_3)/U]^2\} \quad (6)$$

where $v = L/\Delta Z$

light gas plus coke outlet concentration

$$\bar{C}_C = \bar{C}_{a0}{}^2\Delta Z B/U\left[\sum_{j=1}^{v-1} FS_C k_3/[1 + (v-j)B\Delta Z F\bar{C}_{a0}(k_1 + k_3)/U]^2 + \sum_{j=1}^{v-1}\frac{\Delta Z B}{U}k_1 S_G k_2 S_{GC}\sum_{i=1}^{j}\{(1 - B\Delta Z k_2/U)^{i-1}/[1 + (j-i)B\Delta Z F\bar{C}_{a0}(k_1 + k_3)/U]^2\}\right] \quad (7)$$

The set of equations was applied to each gas oil injection of each run. This was achieved by using a computer program, where all data from different flows were treated

with a Marquardt nonlinear regression technique, obtaining the best kinetic parameters fitting the experiment data. In this way, a set of kinetic constants as a function of catalyst time-on-stream was obtained, and the catalyst decay function was then directly derived from these results.

It has to be pointed out that the ratio between the weight of the catalyst and the volumetric flow of the carrier or the ratio between a differential amount of catalyst and the volumetric carrier flow is equivalent to the $B\Delta Z/Uv$ or $B\Delta Z/U$ groups, respectively. The weight of the catalyst and the carrier flow being determined for each of the runs, these parameters were used directly for the definition of B. There was no need of additional information for data analysis.

In the five-lump model, the gas oil feedstock was split in three groups. This model considers that the hydrocarbon compounds forming the feedstock have different functional groups with different crackability characteristics and that these groups behave differently in a model for catalytic cracking reactions. The five-lump model is shown in Figure 2b with three groups of parallel reactions. Following this scheme, the feed components (paraffins, naphthenes, and aromatics) decompose to gasoline and light gases plus coke. This model also includes an additional step for the gasoline cracking into light gases plus coke.

The partial differential equations for this model are similar to the ones developed for the three-lump model except that the order of the reaction for all lumps is one. This condition eliminates the need for the F correction factor when applying the Laplace transformation. The differential equations are reformed in finite difference equations with the same methodology followed in the development of the three-lump model. Then the outlet concentrations for paraffins, naphthenes, and aromatics are the following:

$$\bar{C}_i = \bar{C}_{i0} e^{-(k_{i1}+k_{i3})BL/U} \tag{8}$$

The outlet concentration for gasolines is given by

$$\bar{C}_G = (B\Delta Z/U)\sum_{j=0}^{v-1}[(1 - B\Delta Z k_2/U)^j \sum_{i=1}^{p}(S_{iG} k_{i1} \bar{C}_{i0}) e^{(j+1-v)s'}] \tag{9}$$

The outlet concentration for the gas plus coke lump is given by

$$\bar{C}_C = (B\Delta Z/U)\sum_{j=0}^{v-1}(\sum_{i=1}^{p} S_{iC} k_{i3} \bar{C}_{i0}) \bar{e}^{js'} + \{[(B\Delta Z/U)^2 S_{GC} k_2] \sum_{j=0}^{v-2}(\sum_{i=1}^{p} S_{iG} k_{i1} \bar{C}_{i0} e^{-js'})\} + [(B\Delta Z/U)^2 S_{GC} k_2] \sum_{h=1}^{v-2}\{(1 - B\Delta Z k_2/U)^h [\sum_{j=0}^{v-h-2}(\sum_{i=1}^{p} S_{iG} k_{i1} C_{i0} e^{-js'})]\} \tag{10}$$

where

$$s' = B\Delta Z(k_{i1} + k_{i3})/U$$

This set of five equations was solved for each gas oil pulse to obtain different kinetic parameters. This was achieved through a computer algorithm which also used a Marquardt data fitting technique.

4. Results and Discussion

Figure 3 presents the conversion levels of the different catalysts (Super Nova D, Octacat, GX-30, and Octex) with

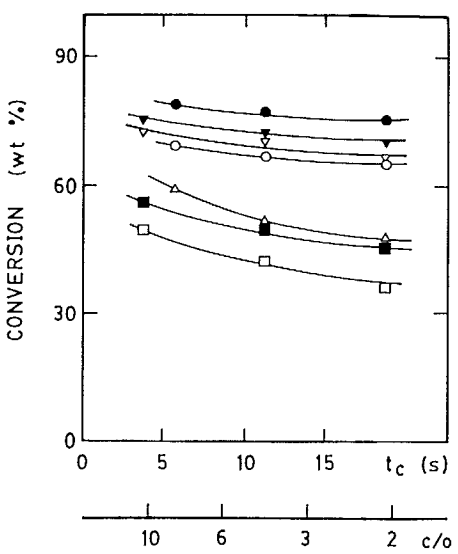

Figure 3. Overall conversion curves for the three catalysts tested at two temperature levels and carrier gas flow (120 std mL/min): (○) Super Nova D, 783 K, SF gas oil; (●) Super Nova D, 823 K, SF gas oil; (□) Octacat, 783 K, SF gas oil; (■) Octacat, 823 K, SF gas oil; (△) Octex, 783 K, PF gas oil; (▽) GX-30, 783 K, SF gas oil; (▼) GX-30, 823 K, SF gas oil.

increasing cumulative contact time or decreasing catalyst-to-oil ratio. Contact times were estimated from the time difference between the feedstock and product peaks obtained from the TCD detectors. As can be observed, conversion decreases with the increment of the cumulative contact time, due to the increasing presence of coke on the catalyst. Since there is only catalyst mixing in between injections and no regeneration of the catalyst, coke starts accumulating uniformity on the catalyst particles, reducing its activity and thus lowering the overall conversion. Conversion also decreases with decreasing catalyst-to-oil ratio, as would be expected.

It has to be pointed out that the catalyst-to-oil ratio, shown as a cumulative value, decreases with the number of gas oil injections, because of the constant weight of catalyst in the bed and the increasing amount of reacted hydrocarbons.

Conversion levels were higher at higher temperatures. This consistent behavior for Super Nova D, GX-30, and Octacat is in agreement with published results that show that at higher temperatures the reaction and kinetic parameters are higher and thus the overall conversion is increased. Octex catalyst (OTX) showed similar trends, with conversion values intermediate between Octacat and Super Nova D (Larocca, 1988). The curves in Figure 3 were obtained from the runs at 120 std mL/min, which was the carrier gas flow chosen as a reference for calculations. However, to provide a complete description of the experimental results, the values of the individual runs at the three different flows are presented in detail in Table III. One imporant observation is that the conversion values for Octacat (OCT) catalyst are lower than those obtained from GX-30 (GX) and Super Nova D (SND). This is because of the basic differences between these catalysts. Although the three of them are manufactured to improve the octane number and to produce a minimum amount of coke, they are based on different formulations: Super Nova D and GX-30 are alumina-based catalysts, whereas Octacat is a silica-based catalyst. Due to the higher unit cell size and the alumina content of Super Nova D and GX-30 (McElhiney, 1988), it is expected that Super Nova D and GX-30 are more active to crack hydocarbon molecules than Octacat, giving a higher overall conversion.

Table III. Overall Conversions from Catalysts Studied (wt %)

run	flow, std mL/min	injection 2	3	6	10
SND, 783 K	120		69.2	67.0	65.9
	135		67.8	65.2	63.7
	150		62.1	62.5	61.1
SND, 823 K	120		77.7	76.8	75.5
	135		77.6	74.4	71.2
	150		71.8	70.5	61.8
OCT, 783 K	120	49.4		42.3	36.5
	135	47.9		32.9	35.4
	150	42.7		35.3	31.8
OCT, 823 K	120	55.5		49.4	45.1
	135	54.2		48.3	43.2
	150	50.8		44.5	40.4
OTX, 783 K	120		67.0	62.2	55.4
	135		62.1	59.6	54.7
	150		59.1	55.8	48.7
GX, 783 K	120	72.1		69.1	66.6
	135	70.4		67.3	64.6
	150	67.8		65.4	62.2
GX, 823 K	120	75.1		72.3	70.3
	135	73.4		71.9	70.0
	150	72.9		70.2	68.9

The variation in light gas (C_1–C_4) production from the experimental runs is presented in Figure 4, which shows an increasing production of light gases with conversion. Furthermore, the temperature increment from 783 to 823 K increases the production of light gases. A temperature increment increases intramolecular motion and intermolecular interactions, assisting the transformation of reactants into new compounds and enhancing the rate of the cracking process (Montgomery, 1970). This temperature effect applies to both primary and secondary reactions, explaining as a consequence the higher light gas yields for higher temperatures. Octacat produces more light gases, at equivalent conversion, than Super Nova D and GX-30, while Octex presents again intermediate values in between the two Davison catalysts.

Gasoline yields are presented in Figure 5 and Table IV, where gasoline was defined as all hydrocarbons in the range 5–12 carbon atoms. An increment in temperature reduces consistently the gasoline selectivity, because at higher temperatures and equivalent conversion the heavy and highly aromatic feed tends to form more coke and gases and less light gasoline. Octacat catalyst produced slightly less gasoline than Super Nova D and GX-30, while GX-30

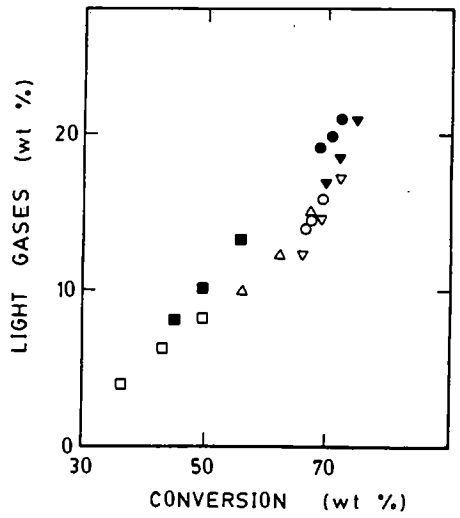

Figure 4. Light gas (C_1–C_4) yield changes with gas oil conversion. For symbols, refer to Figure 3.

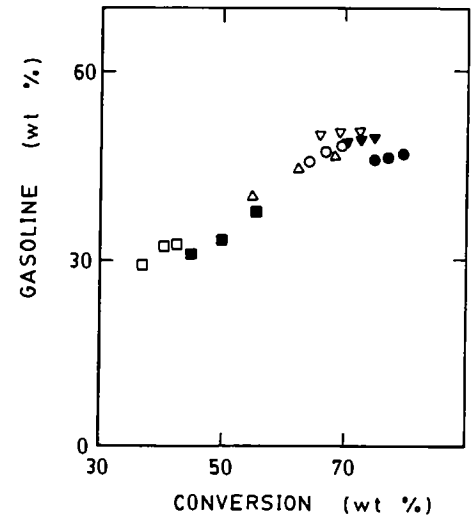

Figure 5. Gasoline yield changes with gas oil conversion. For symbols, refer to Figure 3.

showed the higher gasoline yields. However, the research octane number calculated according to Anderson's method (Anderson et al., 1972) gave a value of 96 for Octacat and 90 for Super Nova D, confirming the characteristics of

Table IV. Coke, Light Gases, and Gasoline Yields (wt %)

run	flow, std mL/min	coke av per injection	light gases injection 2/3	6	10	gasoline injection 2/3	6	10
SND, 783 K	120	5.3	15.9	14.9	14.2	47.9	46.8	46.4
	135	4.0	16.1	15.9	13.3	47.4	48.7	46.4
	150	3.8	14.5	13.7	13.1	44.4	45.0	44.2
SND, 823 K	120	8.1	23.6	22.6	19.9	46.0	46.1	47.5
	135	7.0	23.8	20.3	18.4	46.8	47.2	45.8
	150	6.8	22.3	18.7	15.3	42.7	45.1	39.7
OCT, 783 K	120	3.0	8.6	6.5	5.3	32.2	32.8	28.8
	135	2.8	8.8	5.8	3.9	36.4	29.3	28.8
	150	2.6	7.8	5.9	4.2	32.4	26.9	25.0
OCT, 823 K	120	3.6	13.2	10.4	7.9	38.7	35.4	33.7
	135	3.2	12.9	10.3	8.5	38.2	34.8	32.2
	150	2.8	12.1	9.3	7.8	35.9	32.4	29.8
OCX, 783 K	120	4.9	15.0	12.0	10.5	47.1	45.4	40.0
	135	4.5	13.8	12.8	10.2	46.5	44.9	42.2
	150	3.5	13.4	11.8	9.2	43.5	42.4	37.6
GX, 783 K	120	3.2	17.6	14.8	12.2	51.3	51.1	50.8
	135	2.8	17.2	14.2	12.8	50.4	50.3	49.0
	150	2.6	16.2	13.8	12.0	49.0	49.0	47.6
GX, 823 K	120	4.3	21.1	18.6	16.8	49.7	49.4	49.2
	135	3.8	20.4	17.9	16.3	49.2	50.2	49.9
	150	3.2	20.4	17.3	15.9	49.3	49.7	49.8

Table V. Individual and Overall Gas Oil Cracking Kinetic Constants from Three-Lump Model ($10^{-6}k$, cm^6/(mol•g of Catalyst•s))[a]

run	injection	k_1	k_3	$k_1 + k_3$
SND, 783 K	3	170	74	244
	6	150	70	220
	10	142	67	209
SND, 823 K	3	250	167	417
	6	240	154	394
	10	238	132	320
OCT, 783 K	2	68	26	94
	6	66	20	86
	10	53	15	68
OCT, 823 K	2	120	47	167
	6	91	38	129
	10	81	29	110
OTX, 783 K	3	125	54	179
	6	106	38	144
	10	80	28	108
GX, 783 K	2	240	93	333
	6	211	77	288
	10	180	72	252
GX, 823 K	2	265	129	394
	6	231	112	343
	10	211	102	313

[a] Runs with SND, OCT, and GX were conducted with SF gas oil. Runs with OTX were conducted with PF gas oil.

improved octane number for Octacat catalyst.

Since the gas oil cracking can be modeled with a triangular scheme involving three parameters, the gas oil conversion can be viewed as a competitive reaction. An overall rate constant for gas oil transformation can be defined such that this constant is the sum of the kinetic constants for the gas oil decomposition to gasoline (k_1) and the gas oil cracking to gas plus coke (k_3). Then, the overall kinetic constant can be considered as k or $k_1 + k_3$.

The k values assessed with eq 3 are presented in Table V. Furthermore, the individual values of these constants are also shown in Table V. It has to be pointed out that the value for the calculated kinetic constant for the gasoline decomposition, k_2, was zero or very close to zero. This problem was investigated as follows: with a preset value of k_2, the logarithmic ratio of k_1 and k_3 was evaluated at three different flows. At the conditions where the three lines intercept, a single set of parameters provides the solution of the system. The three curves obtained clearly show that the simultaneous solution of the system of equations at the intersection of the three lines gives a value for k_2 of zero or very close to zero. These results were not surprising; on the contrary, a behavior like this was expected, because other results available in the literature pointed already toward a very small value for the gasoline decomposition kinetic constants (Nace et al., 1971; Weekman, 1968; Corella et al., 1985; Kraemer, 1987; Kraemer and de Lasa, 1988). It was concluded then that in the microcatalytic unit there was essenitally no gasoline overcracking, and the light gases (C_1–C_4) plus coke formed were originated essentially from gas oil cracking. Then, under these conditions, the triangular scheme is simplified in a parallel reaction system with two main transformations taking place: conversion of gas oil to gasoline and conversion of gas oil to light gases plus coke.

The computer program for the three-lump model estimated the values of the kinetic constants, comparing and minimizing the difference between calculated and experimental outlet concentrations. The agreement between these values was very good for the unconverted gas oil, gasoline, and light gases plus coke lumps. For Super Nova D, standard deviations between experimental and predicted amounts for unconverted gas oil, gasoline, and light gases plus coke were ±13.2%, ±11.5%, and ±19%, respectively. For Octacat, these values were ±4.7%, ±6.4%, and ±11.4%, respectively. Deviations found for Octex and GX-30 were ±5–6%, ±5–6%, and ±11–12%. This confirms that the three-lump model, as considered in the present study, provided a good representation of gas oil catalytic cracking.

In Table V, it can be observed how the change in temperature increases the value of the kinetic constants. Super Nova D and GX-30 show values higher than Octacat, reflecting the observed difference in conversion levels. Also it is important to note the decrement of the kinetic constants with the number of injections. In fact, as the coke deposited on catalyst increases, the hydrocarbon cracking becomes more difficult, and this is reflected in a reduction of the kinetic parameters.

From the individual values of the kinetic constants presented in Table V, it can be observed that the cracking rate constant for the gasoline is more than double with respect to the one for light gases plus coke formation. This ratio is well in the range of k_1/k_3 values reported in the literature, which go from 1 to 5 (Nace et al., 1971; Weekman, 1968; Corella et al., 1985; Kraemer, 1987). The k_1/k_3 ratio is higher for Octacat, evidencing the minimum coke selectivity characteristics of this catalyst (Davison, 1984, 1985, 1987a,b).

The results of the computer program for the five-lump model in the cases of Octacat, GX-30, and Super Nova D gave a total of six kinetic constants, two for each one of the groups originated from the feed, paraffins, naphthenes, and aromatics. With these constants, the simulation gave as a result the calculated values for unconverted materials and yields of gasoline and light gases plus coke. The comparison between experimental and calculated values for the unconverted lumps is quite good except for the paraffins. For example, for Super Nova D, standard deviations between observed and predicted lump yields are as follows: ±21.6% for the paraffinic lump, ±14.9% for the naphthenic lump, ±12.5% for the aromatic lump. Then, the standard deviation is about ±20% for paraffins, much larger than the ±12–14% obtained for naphthenes and aromatics. Similar results were obtained for Octacat with standard deviations of ±15.8% for the paraffinic lump, ±11% for the naphtenic lump, and ±9.5% for the aromatic lump. This may be explained, as reported in Table II, by the small amount of paraffins present (about 7%) in the SF gas oil used in these experimental runs.

However, the experimental results for unconverted paraffins with Octex were in quite good agreement with the calculated values (standard deviation: ±4.5%). For this catalyst, a different gas oil, PF instead of SF, highly paraffinic, was used as a feedstock. So it is reasonable to assume that the accuracy of the procedure, in the case of the cracking of an aromatic feedstock on Super Nova D, GX-30, and Octacat catalysts, was responsible for the bigger deviations observed in the prediction of the unconverted paraffinic lump.

The overall and individual lump kinetic constants are presented respectively in Tables VI, Table VII, and VIII. The trends observed are similar to the ones described for the results of the three-lump model. The overall and individual kinetic constants for the three lumps decreased with time-on-stream and increased with temperature. The only exception was the individual kinetic constants for the paraffinic lumps, the cases of Super Nova D, GX-30, and Octacat. As mentioned above, this was attributed to the lower reliability of determining kinetic properties based

Table VI. Overall Gas Oil Lump Cracking Kinetic Constants ($k_{12} + k_{13}$, cm³/(g of Catalyst • s))[a]

run	injection	lump paraffinic	lump naphthenic	lump aromatic
SND, 783 K	3	16.5	25.4	23.3
	6	12.9	24.1	22.3
	10	11.6	23.1	22.1
SND, 823 K	3	21.0	33.2	32.2
	6	19.6	32.0	31.6
	10	19.3	31.7	29.7
OCT, 783 K	2	18.6	8.3	14.8
	6	14.1	8.1	14.3
	10	10.5	7.1	11.6
OCT, 823 K	2	24.6	17.8	17.2
	6	18.9	13.1	16.2
	10	15.6	13.0	13.2
OCX, 783 K	3	24.1	13.3	21.4
	6	21.7	9.2	20.3
	10	18.4	6.2	16.8
GX, 783 K	3	21.6	31.9	25.6
	6	17.1	30.3	23.4
	10	11.8	28.6	22.1
GX, 823 K	3	23.1	32.8	29.8
	6	20.0	33.2	25.9
	10	16.9	32.8	24.1

[a] Runs with SND, OCT, and GX were conducted with SF gas oil. Runs with OTX were conducted with PF gas oil.

Table VII. Individual Lump Cracking Kinetic Constants (cm³/(g of Catalyst • s))[a]

temp, K	783	783	783	823	823	823
injection	2/3	6	10	2/3	6	10
			Super Nova D			
k_{P1}	4.5	7.7	6.3	14.7	0.0	15.7
k_{P3}	9.2	3.7	0.0	9.4	19.6	1.5
k_{N1}	18.5	18.4	17.2	19.2	19.0	19.2
k_{N3}	7.4	6.9	6.9	13.8	12.1	11.8
k_{A1}	18.0	17.2	16.0	22.6	22.2	19.4
k_{A3}	6.0	6.8	5.9	11.8	8.7	9.8
			Octacat			
k_{P1}	15.3	7.7	9.6	1.9	5.8	3.8
k_{P3}	0.0	4.9	0.1	18.2	12.2	11.1
k_{N1}	8.3	9.6	4.6	15.3	12.4	9.3
k_{N3}	4.0	0.2	2.4	3.6	2.5	2.7
k_{A1}	10.3	7.9	9.8	12.2	10.6	10.9
k_{A3}	3.4	4.4	2.1	4.6	4.5	2.8
			GX-30			
k_{P1}	12.4	9.7	7.2	21.7	18.6	15.6
k_{P3}	9.2	7.4	4.6	1.4	1.5	1.3
k_{N1}	20.9	20.1	18.7	19.7	20.2	19.8
k_{N3}	11.9	10.2	9.9	11.8	9.7	9.5
k_{A1}	19.9	18.2	17.2	20.6	18.2	17.2
k_{A3}	5.7	5.2	4.9	8.6	7.6	7.0

[a] Runs were conducted with SF gas oil.

Table VIII. Individual Lump Cracking Kinetic Constants for Octex (cm³/(g of Catalyst • s))[a]

temp, K	783	783	783
injection	3	6	10
k_{P1}	16.6	14.8	12.9
k_{P3}	7.2	6.6	5.3
k_{N1}	8.0	7.1	4.0
k_{N3}	3.9	1.4	1.0
k_{A1}	17.5	17.1	16.7
k_{A3}	2.5	1.1	0.1

[a] Runs were conducted with PF gas oil.

on a smaller fraction of paraffins.

From the runs for Super Nova D and Octacat, it was also possible to estimate the activation energy for the cracking reactions. These values are in the range of energies of activation reported in the literature (Decroocq, 1984; Wollaston and Haflin, 1975; Weekman, 1979). From the runs with GX-30 a lower activation energy, 25.3 ± 3.8 kJ/mol, was obtained. Low energies of activation may point, as stated by Chen and Lucki (1986) and Collyer et al. (1988), toward intraparticle diffusional limitations in the GX-30 catalyst. It has to be pointed out that this low energy of activation is consistent with values obtained by Kraemer and de Lasa (1988) and Collyer et al. (1988). Furthermore, the GX-30 catalyst, the catalyst with the lower energy of activation, was also the one with the biggest unit cell size, which may be a main contributing factor for a very reactive diffusionally controlled catalyst (Leuenberger et al., 1988).

In our study, the deactivation of the catalyst due to the coke buildup was first represented by a power function of the following type:

$$k = k_0 t_c^{-m} \tag{11}$$

where k_0 is the initial rate constant, t_c is the cumulative catalyst time-on-stream, and m is an exponent, which is directly related to the deactivation occurring at specific conditions

$$m = 1/(n-1) \qquad \text{for} \quad n > 1 \tag{12}$$

where n is the order of decay, as it appears in the general expression for the rate of catalyst activity decay:

$$-dX/dt = k_c X^n \tag{13}$$

In eq 11, X represents the fraction of sites available at any time t, k_c is a kinetic constant, and n is the order of reaction.

The power decay function presented in eq 11 has been found to be valid for experimental data obtained approximately below 60 s for catalyst time-on-stream (Nace, 1970, Corella et al., 1985; Habib et al., 1977; Weekman, 1968, 1979; Voltz et al., 1971; Jacob et al., 1976). However and because of the shorter catalyst time-on-stream in riser reactors (below 20 s), a more in-depth analysis of the problem was required. The special design of the pulse microcatalytic reactor proposed in this study allowed coverage of this range of catalyst time-on-stream.

The experimental results of this investigatin, as described above, allowed assessment of kinetic constants (k) from the three-lump model at different times-on-stream (Table V). This gave for the three catalysts studied, Super Nova D, GX-30, and Octacat, average values of 0.10, 0.15, and 0.22, respectively, for the exponent m. This is equivalent, applying eq 12, between a fifth to ninth order of deactivation. This basically means that in the time scale of the riser reactor (<20 s), for each deactivating event, a total of five active sites are lost for further cracking. This seems to be true at least until regeneration occurs and coke is removed from the surface by combustion. Since common values for m are in the range 0.2–0.5 (Nace, 1970; Corella et al., 1985), and since the deactivation order increases with the coke-forming potential of the feedstock (Nace, 1970), then the average m values obtained in this study are quite reasonable, considering the high aromatic content of the gas oil used during the cracking runs. This is especially true if one considers that the paraffinic gas oil used in other investigations gave values of m higher than 0.25 (Nace, 1970).

It must be noted that a critical comparison of the results of this study in terms of the m exponent is quite difficult. This is due to the lack of information in the literature about catalytic cracking under short catalyst times-on-stream, necessary to mimic riser reactors. In fact, cracking data were usually obtained at catalyst times-on-stream

higher than 20 s, and the results were frequently fitted with the exponential decay law or the mathematical equivalent condition of $m = 1$ (Gross et al., 1974; Newson, 1975; Nace, 1969a,b, 1970; Mann et al., 1986; Mann and Thomson, 1987; Tan and Fuller, 1970; Voltz et al., 1971; Weekman, 1968).

It can certainly be speculated that, as the catalyst time-on-stream increases, the average number of active sites neutralized in each deactivating event decreases until eventually it reaches the value of one, for which eq 11 will give as a result of integration the frequently proposed exponential decay function.

Nace (1970) studied this problem, gathering data in the range 10–150 s of catalyst time-on-stream in a continuous unit. Even if the adequacy of the unit, similar to the MAT test, could be questioned, due to the coke profile created in the bed, a good data fit with the power decay law with exponents ranging from 0.2 to 0.4 was obtained. It should be mentioned that Nace (1970) also found that m values depended on the type of feedstock.

The theoretical model used for the interpretation of the experimental results considers that the specific activity of all sites on a given catalyst is uniform. However, researchers have also approached this problem from another viewpoint, assuming the existence of active sites of different strength (Corella et al., 1985), which means that the catalyst has a nonhomogeneous surface, where active sites have different acidity, depending on the degree of isolation of sites from their neighbors (Pine et al., 1984). Under these circumstances, the sites with higher strength are the first ones involved in cracking events and coked at the beginning of a run, because of their higher acidity. Then, following this view, the sites with lower strength would be available, once the first gorup of more active sites are coked. In this case, there is the possibility to use, as suggested by Corella et al. (1985), a mathematical representation of the change of the kinetic constants based on a summation of exponentials with different decay coefficients. The exponential terms for the stronger active sites, having the bigger decay coefficients, should have a dominant effect for the first few seconds of catalyst time-on-stream. Following this, the stronger sites will be coked and the weaker sites will dominate the catalyst operation both in terms of conversion, selectivity to gasoline, and coke fermentation (Collyer et al., 1988). Considering these facts, there is a definite possibility that a single exponential corresponding to the change of activity for the stronger sites could correlate very well the changes of catalytic activities in a riser unit (Kraemer and de Lasa, 1988). On this basis, the global kinetic constants (k) reported in Table V and derived from conversion data, using eq 3, were plotted in a ln k vs t_c graph (Figure 6). This is equivalent to fitting the catalyst decay with an exponential decay model. It can be observed that, even for the short catalyst time-on-stream used in this contribution, a single-exponential decay law provides a very good representation of the data (coefficients of correlation: 0.964–0.999) for the four catalysts tested: Super Nova D, GX-30, Octacat, and Octex. The energies of activation, resulting from the evaluation of the kinetic constant at $t_c = 0$, $-E = 83.17$ kJ/mol for Super Nova D, $-E = 75.05$ kJ/mol for Octacat, $-E = 20.76$ kJ/mol for GX-30, are in the same range as the energies of activation assessed with the power law function (69 ± 10 kJ/mol for Super Nova D, 65 ± 11 kJ/mol for Octacat, and 25.33 ± 3.8 kJ/mol for GX-30).

Consequently, the power law and the exponential decay were revealed as equivalent functions for correlating the data for short contact times in this study. Furthermore,

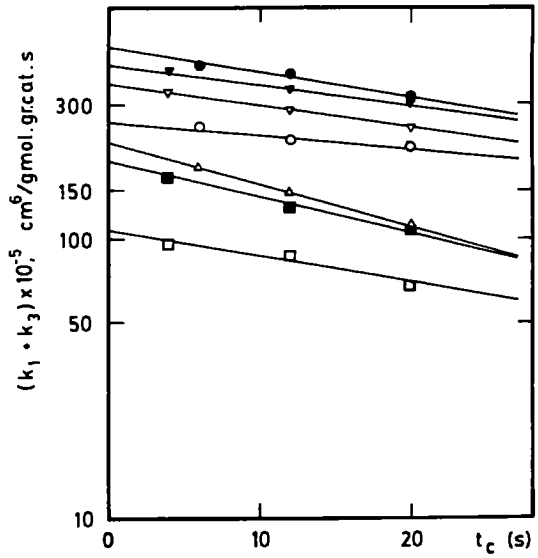

Figure 6. Change of the kinetic constant with the catalyst time-on-stream. Full lines represent the experimental decay model. For symbols, refer to Figure 3.

and because of the adequacy of both deactivation functions tested, it is our view that a relation of these functions with mechanistics events, such as the number of sites involved in the coke formation, cannot be directly inferred from these experiments.

5. Conclusions

Based on the general results obtained during this investigation, it is concluded that the pulse technique with a fixed bed microcatalytic unit has been proven to be quite adequate for the evaluation of cracking catalyst, for the acquisition of reliable yield data for the design of riser units, and for the evaluation of kinetic deactivation parameters. A kinetic model formed by three lumps, i.e., gas oil, gasoline, and light gases plus coke, was used to reproduce the experimental data with success.

An additional kinetic model with five lumps was also implemented to explain the experimental results. The model splits the gas oil into three different basic groups: paraffins, naphthenes, and aromatics, allowing for the evaluation of kinetic reaction rate constants for each individual group. The model reproduced the experimental yields quite well, except for the paraffinic lump in the synthetic feedstock, due to the very low concentration of paraffins.

The catalyst deactivation was evaluated under conditions representative of commercial operations, and it was found that for contact times under 20 s the deactivation process can be represented by a power decay function with an average exponent of 0.1–0.2. By use of the time-on-stream theory of catalyst decay, the average exponent value of the power function found is equivalent to a decay order of nine to five, which according to the postulates of the theory means that in each deactivating event five active sites of uniform activity were involved. The same theory was applied to the results by using an exponential decay function. It was found that the exponential decay law also showed very good ability to correlate the kinetic constants at various times-on-stream. It was concluded, then, that power law and exponential decay functions have equivalent ability for correlating kinetic constant decay under short contact time conditions.

Acknowledgment

The authors acknowledge the guidance and assistance received from CANMET, Energy Research Laboratories, Canada, Davison Chemical Division of W. R. Grace and Co., and Harshaw Filtrol Co.

Nomenclature

B = parameter used for the lump models, kg/m^3
C_a = gas oil concentration, kmol/m^3
C_{a0} = initial gas oil concentration, kmol/m^3
C_C = coke plus light gas concentration, kmol/m^3
C_G = gasoline concentration, kmol/m^3
$\bar{C}_a$ = Laplace gas oil concentration at $s = 0$, (kmol·s)/m^3
$\bar{C}_{a0}$ = initial Laplace gas oil concentration at $s = 0$, (kmol·s)/m^3
$\bar{C}_C$ = Laplace transform of gas + coke concentration, (kmol·s)/m^3
$\bar{C}_G$ = Laplace transform of gasoline concentration, (kmol·s)/m^3
$\bar{C}_i$ = Laplace transform of "i" lump concentration, (kmol·s)/m^3
$\bar{C}_{i0}$ = Laplace transform of "i" lump concentration at reactor entry, (kmol·s)/m^3
F = Laplace correction factor, 1/s
f = dilution factor, kg of catalyst/kg of bed
k = global gas oil cracking kinetic constant for three-lump model, m^6/(kmol·kg of catalyst·s)
k_c = constant parameter in eq 11, 1/s
K_a = adsorption constant, m^3/kg
k_1 = individual kinetic constant for gas oil cracking to gasoline in the three-lump model, m^6/(kmol·kg of catalyst·s)
k_2 = individual kinetic constant for gasoline cracking to light gas plus coke in three-lump model, m^3/(kg of catalyst·s)
k_3 = individual kinetic constant for gas oil cracking to gas plus coke in three-lump model, m^6/(kmol·kg of catalyst·s)
k_{i1} = kinetic constant for lump "i" cracking to gasoline, m^3/(kg of catalyst·s)
k_{i3} = kinetic constant for lump "i" cracking to gas plus coke, m^3/(kg of catalyst·s)
k_{A1} = kinetic constant for aromatic cracking to gasoline m^3/(kg of catalyst·s)
k_{A3} = kinetic constant for aromatic cracking to gas plus coke, m^3/(kg of catalyst·s)
k_{N1} = kinetic constant for naphthene cracking to gasoline, m^3/(kg of catalyst·s)
k_{N3} = kinetic constant for naphthene cracking to gas plus coke, m^3/(kg of catalyst·s)
k_{P1} = kinetic constant for paraffin cracking to gasoline, m^3/(kg of catalyst·s)
k_{P3} = kinetic constant for paraffin cracking to gas plus coke m^3/(kg of catalyst·s)
L = reactor length, m
m = decay exponent in eq 10
n = number of active sites taking part in deactivating event in eq 11
r_a = gas oil rate of cracking, kmol/(kg of catalyst·s)
s' = parameter for five-lump model
S_C = gas + coke stoichiometric coefficient
S_G = gasoline stoichiometric coefficient
S_{GC} = gasoline to C lump stoichiometric coefficient
S_{iC} = lump "i" to lump C stoichiometric coefficient
S_{iG} = lump "i" to gasoline stoichiometric coefficient
T = temperature, K
t = time, s
t_c = catalyst–oil contact time, s
U = gas linear velocity, m/s
v = constant parameter for lump models
X = fraction of active sites available on catalyst at any time t
z = reactor height, m

Subscript

i = 1, 2, 3, refers to the paraffinic, aromatic, or naphthenic lumps

Greek Symbols

ϵ = intergranular porosity, m^3 of void/m^3 of bed
ϵ_p = intragranular porosity, m^3 of void/m^3 of pellet
ρ_p = particle bulk density, kg/m^3
Δ = finite difference in differential equations

Catalysts

OCT = Octacat
OTX = Octex
SND = Super Nova D
GX = GX-30

Registry No. Carbon, 7440-44-0.

Literature Cited

Anderson, P. C.; Sharkey, J. M.; Walsh, R. P. Calculations of the research octane number of motor gasolines from gas chromatographic data and a new approach to motor gasoline quality control. *J. Inst. Pet.* **1972**, *58*, 560.

Chen, N. Y.; Lucki, S. J. Nonregenerative Catalytic Cracking of Gas Oils. *Ind. Eng. Chem. Process Des. Dev.* **1986**, *25*, 814.

Collyer, R.; de Lasa, H.; Larocca, M. Modelling the Kinetics of Fast Catalytic Cracking Reactions. *Can. J. Chem. Eng.* **1988**, in press.

Corella, J.; Bilbao, R.; Molina, J.; Artiga, A. Variation with time of the mechanism observable order, and activation energy of the catalyst deactivation by coke in the FCC process. *Ind. Eng. Chem. Process Des. Dev.* **1985**, *24*, 625.

Davison. Davison Octacat meets the challenge. Catalagram No. 69, 1984.

Davison. Davison's coke selective fluid cracking catalysts. Catalagram No. 73, 1985.

Davison. FCC catalyst technology update. Technical Service Department Seminar, Jan 1987a.

Davison. A new era for the coke-selective catalyst. Catalagram No. 75, 1987b.

Dean, J. W.; Dadyborjor, D. B. Activity and Coke Deposition on a Composite Acid Catalyst and Its Components. *Ind. Eng. Chem. Res.* **1989**, *28*, 271.

Decroocq, D. *Catalytic cracking of heavy petroleum fractions*; Gulf Publishing Company: Houston, TX, 1984.

de Lasa, H. Fluidized bed catalytic cracking technology. *Lat. Am. J. Chem. Eng. Appl. Chem.* **1982**, *12*, 171.

El-Kady, F. Y. A.; Mann, R. Fouling and deactivation of a FCC catalyst I. *Appl. Catal.* **1982a**, *3*, 211.

El-Kady, F. Y. A.; Mann, R. Fouling and deactivation of a FCC catalyst II. *Appl. Catal.* **1982b**, *3*, 235.

Forzatti, P.; Buzzi, G.; Morbidelli, M.; Carra, S. Deactivation of catalyst. 1. Chemical and Kinetic aspects. *Int. Chem. Eng.* **1984**, *24*, 1.

Froment, G. F.; Bischoff, K. B. Non-steady state behavior of fixed bed catalytic reactors due to catalyst fouling. *Chem. Eng. Sci.* **1961**, *16*, 189.

Froment, G. F.; Bischoff, K. B. Kinetic data and product distribution from fixed bed catalytic reactors subject to catalyst fouling. *Chem. Eng. Sci.* **1962**, *17*, 105.

Fuentes, G. A. Catalyst deactivation and steady state activity: a generalized power law equation model. *Appl. Catal.* **1985**, *15*, 33.

Gross, B.; Nace, D.; Voltz, S. E. Application of a kinetic model for comparison of catalytic cracking in a fixed bed microreactor and a fluidized dense bed. *Ind. Eng. Chem. Process Des. Dev.* **1974**, *13*, 3.

Habib, E. T.; Owen, H.; Venuto, P. B. Artificially metal poisoned fluid catalysts. Performance in pilot plant cracking of hydrotreated resid. *Ind. Eng. Chem. Prod. Res. Dev.* **1977**, *16*, 4.

Jacob, S. M.; Gross, B.; Voltz, S.; Weekman, V. W. A lumping and reaction scheme for datalytic cracking. *AIChE J.* **1976**, *22*, 4.

Kraemer, D. Catalytic cracking of hydrocarbons in a riser simulator: design and testing. Master of Eng. Thesis, University of Western Ontario, London, Ontario, Canada, 1987.

Kraemer, D.; de Lasa, H. Catalytic Cracking of Hydrocarbons in a Riser Simulator. *Ind. Eng. Chem. Res.* **1988**, *27*, 2002.

Kraemer, D.; Larocca, M.; de Lasa, H. Deactivation of Cracking Catalyst in Short Time Reactors. *Can. J. Chem. Eng.* **1989**, submitted for publication.

Larocca, M. Fast Catalytic Cracking with nickel and vanadium contaminants. Ph.D. Dissertation, University of Western Ontario, London, Ontario, Canada, 1988.
Leuenberger, E. L.; Moorehead, E. L.; Newell, D. F. Effect of Feedstock Type on FCC Overcracking. 1988 NPRA Annual Meeting, March 20, 1988; AM-88-51.
Mann, R.; Thomson, G. Deactivation of a supported zeolite catalyst: simulation of diffusion, reaction and coke deposition in a parallel bundle. *Chem. Eng. Sci.* **1987**, *42*, 3.
Mann, R.; Sharratt, H. P. N.; Thomson, G. Deactivation of a supported zeolite catalyst: diffusion, reaction and coke deposition in stoichastic pure networks. *Chem. Eng. Sci.* **1986**, *41* (4), 711.
McElhiney, G. FCC catalyst selectivity determined from microactivity tests. *Oil Gas J.* **1988**, *35*, Feb 8.
Meisenheimer, R. G. A mechanism for the deactivation of trace metal contaminants on cracking catalysts. *J. Catal.* **1962**, *1*, 356.
Montgomery, J. A. Catalytic cracking. The effects of operational variables. The Davison Chemical Guide to Catalytic Cracking. Davison Chemical Division, 1970.
Nace, D. M. Catalytic cracking over crystalline alluminosilicates I. *Ind. Eng. Chem. Prod. Res. Dev.* **1969a**, *8*, 1.
Nace, D. M. Catalytic cracking over crystalline aluminosilicates II. *Ind. Eng. Chem. Prod. Res. Dev.* **1969b**, *8*, 1.
Nace, D. M. Catalytic cracking over crystalline aluminosilicates. *Ind. Eng. Chem. Prod. Res. Dev.* **1970**, *9*, 2.
Nace, D. M.; Voltz, S. E.; Weekman, V. W. Application of a kinetic model for catalytic cracking. Effects of charge stocks. *Ind. Eng. Chem. Process Des. Dev.* **1971**, *10*, 530.
Nalltham, R. V.; Tarrer, A. R. Application of a catalyst deactivation model for hydrotreating solvent refined coal feedstocks. *Ind. Eng. Chem. Process Des. Dev.* **1983**, *22*, 645.
Newson, E. Catalyst deactivation due to pore-plugging by reaction products. *Ind. Eng. Chem. Process Des. Dev.* **1975**, *14*, 1.
Pine, L. A.; Maher, P. J.; Wachter, W. A. Prediction of cracking catalyst behaviour by a zeolite unit cell size model. *J. Catal.* **1984**, *84*, 466.
Szepe, S.; Levenspiel, O.; Catalyst deactivation. In *O. Proc. European Fed., 4th Int. Cong. Chem. React. Eng.*; Pergamon Press: New York, 1971.
Tan, C. H.; Fuller, O. M. A model fouling reaction in a zeolite catalyst. *Can. J. Chem. Eng.* **1970**, *48*, 4.
Voltz, S. E.; Nace, D. M.; Weekman, V. W. Application of a kinetic model for catalytic cracking. *Ind. Eng. Chem. Process Des. Dev.* **1971**, *10*, 4.
Voorhies, A. Carbon formation on catalytic cracking. *Ind. Eng. Chem.* **1945**, *37*, 4.
Weekman, V. W. A model of catalytic cracking conversion in fixed, moving, and fluid bed reactors. *Ind. Eng. Chem. Process Des. Dev.* **1968**, *7*, 1.
Weekman, V. W. Lumps, models and kinetics in practice. *AIChE Monogr. Ser.* **1979**, *11*, 75.
Wheeler, A. *Catalysis*; Reinhold: New York, 1955; Vol. 2.
Wojciechowski, B. W. A theoretical treatment of catalyst decay. *Can. J. Chem. Eng.* **1968**, *46*, 2.
Wojciechowski, B. W. The kinetic foundation and practical application of the time on stream theory of catalyst decay. *Cat. Rev. Sci. Eng.* **1974**, *9* (1), 79.
Wolf, E. E.; Alfani, F. Catalyst deactivation by coking. *Cat. Rev. Sci. Eng.* **1982**, *24* (3), 329.
Wollaston, E. G.; Haflin, W. J. What influences cat cracking. *Hydrocarbon Process.* **1975**, *93*, 9.

Received for review March 24, 1989
Accepted October 3, 1989